

1-17-2021

Heat Transfer Characteristics with Internal Heat Generation through Porous Medium.

Gamal Sultan

a Professor at the Department of Mechanical Power Engineering, Mansoura University, Mansoura, Egypt,
gisultan@mans.edu.eg

Follow this and additional works at: <https://mej.researchcommons.org/home>

Recommended Citation

Sultan, Gamal (2021) "Heat Transfer Characteristics with Internal Heat Generation through Porous Medium.," *Mansoura Engineering Journal*: Vol. 29 : Iss. 3 , Article 8.

Available at: <https://doi.org/10.21608/bfemu.2021.140363>

This Original Study is brought to you for free and open access by Mansoura Engineering Journal. It has been accepted for inclusion in Mansoura Engineering Journal by an authorized editor of Mansoura Engineering Journal. For more information, please contact mej@mans.edu.eg.

HEAT TRANSFER CHARACTERISTICS WITH INTERNAL HEAT GENERATION THROUGH POROUS MEDIUM

خواص إنتقال الحرارة في وسط مسامي ذو حرارة داخلية مولدة

G. I. Sultan

Faculty of Engineering, El-Mansoura Univ.,
El-Mansoura, Egypt.

Email: gisultan@mans.edu.eg

الخلاصة:

يتضمن البحث دراسة معملية لإنتقال الحرارة وفقد الضغط لتيار هوائي يسرى في أنبوبة أفقية مملوءة بوسط مسامي ذو حرارة متولدة داخليا. ويتكون الجزء المختبر من أنبوبة نحاسية قطرها الداخلي ٠.٠٢ متر، وطولها ٠.٢٢٥ متر. وخلال التجارب تتغير قيمة المسامية من ٠.٢٥٢٧ إلى ٠.٥٢٥١ وذلك باستخدام كريات من الصلب متساوية القطر. ويتم تسخين الكريات باستخدام الحث الكهربائي من خلال مرور تيار كهربائي متغير في الملف الحثي الملفوف بانتظام حول الأنبوبة النحاسية بعد عزلها كهربيا. وأثناء التجارب كان رقم رينولدز لتيار الهواء يتراوح بين ٢٥٠ & ١٠٦٠٠ بينما كان رقم جراشوف ١.٢ × ١٠^٧. وقد أظهرت النتائج أن معامل الإحتكاك يقل بزيادة رقم رينولدز كما في حالة الموانع النيوتينية، بينما معامل إنتقال الحرارة (رقم نوسلت) يتزايد في هذه الحالة مع زيادة رقم رينولدز وتناقص مسامية الوسط. وقد تم إستنتاج معادلة تجريبية لابعدية لحساب معامل إنتقال الحرارة (رقم نوسلت) كدالة في رقم رايلي ونسبة قطر الكريات إلى قطر الأنبوبة المختبرة، وأيضا علاقة أخرى لابعدية لحساب معامل الإحتكاك كدالة في رقم رينولدز ونسبة قطر الكريات إلى قطر الأنبوبة المختبرة.

Abstract:

Heat transfer and pressure drop were measured for flow of air through a horizontal tube filled with porous media with internal induction heat generation. The heated copper test section has an inside diameter of 0.02 m, and 0.225 m long. The porosity was varied from 0.2527 to 0.5251 using uniform spherical steel beads. These beads are internally heated by passing alternative current through an induction coil wrapped around the tested tube. Over the range of $250 < Re < 10600$, and $Gr = 1.2 \times 10^7$, the friction factor data agreed with the Newtonian prediction. Heat transfer increases with increasing Reynolds number and decreasing porosity. A new experimental correlation were proposed for predicting the heat transfer and friction factor of fluid flow through confined porous media.

Keyword: porous media, heat generation, induction heating.

Nomenclature

A	Surface area, m ²	L	Test section length, m
A _c	Cross-sectional area of test section, m ²	m	Air mass flow rate, kg/s
C _p	Specific heat at constant pressure, J/kg.K	n	No. of thermocouples
d _B	Bead diameter, m	P	Pressure, Pa
D	Test section tube diameter, m	Q	Induction heat generation, W
f	Friction factor	q	Heat flux, W/m ²
g	Gravitational acceleration, m/s ²	T	Temperature, K
h	Convective heat transfer coefficient, W/m ² K	u	Average air velocity, m/s
I	Current intensity, A	V	Voltage drop, V
\bar{k}_a	Air thermal conductivity, W/m K	\dot{V}_a	Air volume flow rate, m ³ /s
k _s	Beads thermal conductivity, W/m.K		

Dimensionless Groups

Da	Darcy number, K/D
Gr	Grashof number, $g\beta\Delta T d_B^3/\nu^2$
Nu	Nusselt number, $h d_B/\bar{k}_a$
Pr	Prandtl number, $C_p\mu/k_a$
Ra	Rayleigh number, $g\beta\Delta T k d_B/\nu\alpha$
Re*	Modified Reynolds number, $\rho_a u d\beta/\mu(1-\phi)$

Greeks

ρ	Density, kg/m^3
ϕ	Porosity
μ	Dynamic viscosity, kg/m.s
β	thermal expansion coeff., $1/\text{K}$
ν	Kinematic viscosity, m^2/s
α	Thermal diffusivity, m^2/s

Subscripts

av	average
c	Cross-sectional area
e	exit
i	inlet
ex	experimental
o	ambient
p	predicted
wi	Wall local

1. Introduction

Fluid flow and heat transfer through porous substances is of great interest in many fields such as chemical engineering, flow in packed columns, regeneration of catalysts, in petroleum engineering,etc. A great deal of research work has been devoted during the past decades to understand the convective heat transfer through porous media.

Moalem (1976), made a theoretical analysis of internally energised porous reactor assuming constant and temperature dependent rate of heat generation. Fluid passed through the heated porous element medium changes phase from liquid to vapor. It is found that in a steady state operation, the use of temperature dependent rate of heat generation might cause a significant decrease in the possible mass flux through the element. Tveiterid (1977), proposed a steady state solutions in the form of hexagons and two-dimensional rolls for convection in a horizontal porous layer heated internally. He found that down-hexagons are stable for Rayleigh number up to 8 times the critical value, while up-hexagons are unstable for all values of Rayleigh number. Decker and Glicksman (1983) proposed a physical model for heat transfer to immersed surfaces in large particle fluidized beds. They found that as

particle size increases the heat transfer by gas convection provides a greater share of the heat transfer. Catton and Jakobsson (1987), investigated experimentally the effects of pressure on dryout heat flux in a volume heated porous bed. The beds were saturated with water, R113, acetone, and methanol. Stewart et al. (1994), modeled two new strong bin designs using a permeable annulus along the centerline of the bin. They found that the maximum and average temperatures for a heat generation rate of 10 W/m^2 and ambient air temperature of 15.5°C . Gobin et al. (1998), Studied theoretically the natural convection driven by combined thermal and solutal buoyancy forces in a binary fluid. Their results showed a significant influence of the presence of a relatively thin porous layer on the flow structure. Also, the effect of permeability on the behavior of the flow structure and average heat transfer is investigated. Calmidi and Mahajan (2000), studied experimentally and numerically forced convection in high porosity aluminum metal foam ($0.89 \leq \phi \leq 0.97$). Their results indicated that for foam-air combinations, the transport enhancing effect of thermal dispersion is extremely low due to the relatively high conductivity of the solid matrix. Meanwhile for foam-water combinations, the results indicated that

thermal dispersion can be very high and accounts for bulk of the transport. Bemacer et al. (2001), focused his study on double-diffusive natural convection in a square cavity filled with porous media heated and cooled along vertical walls by uniform heat fluxes when a solutal flux is imposed vertically. They found three distinct regimes which are called fully thermal convective regimes in which the flow is essentially due to thermal boundary force, diffusive regime where the solutal forces are strong enough to produce a stable solutal stratification with no significant convective flow, and an intermediate regime where a hysteresis is observed. The study included the effect of Ra, Lewis, and Darcy numbers on the flow regimes. Lee

(2001), studied theoretically three different configuration of fluid-particle system to find the sensitivity of heat transfer capabilities with respect to operating parameters such that as fluid velocity and particle packing type. He found that constant volumetric heat source for the column was considered assuming that non-uniform local effects on heat generation of the CST "Crystalline Silicitanate" particles are negligible. He also concluded that the coolability of the packed column containing volumetric heat source under process flow condition is much higher than the CST column with no flow. Mozhaev and Polyayev (2002), investigated experimentally an semiempirical model of heat transfer in non-uniform porous media of internal heat transfer. They reported a dimensionless correlation of heat transfer for the motion of a single phase cooler and the classification of the regimes of internal heat transfer in non-ordered porous structures as a function of Reynolds number is suggested. Raffray et al. (2002), proposed innovative techniques using porous media heat transfer in filtered by the coolant. Developing improved

phenomenological thermal-hydraulic models in order to explain various porous heat transfer media and to help optimize the heat transfer coefficient while minimizing the

associated fluid friction. Rao (2002), studied experimentally the heat transfer and pressure drop for flow of a gaseous solutions of Carbopoi 934 and Carbopoi EZI through a vertical electrically heated stainless steel tube filled with porous media. He found that heat transfer increases with increasing Reynolds number, Prandtl number and increasing porosity. A new correlation is obtained for predicting the heat transfer through the confined porous media. Khalili et al. (2002), studied theoretically the convective instabilities caused by a nonuniform temperature gradient due to vertical through flow and internal heat generation through anisotropic porous layer. They found that an increase in ratio of effective thermal diffusivity to permeability increases the stability of the system. Also, they found that if an internal heat source exists, through flow destabilize the system irrespective of the boundary types considered.

From the last literature review, a lot of research work is concerned in porous media and packed bed but a very little work is concerned on heat generation through porous media. So, the aim of this study is concerned with fluid flow and heat transfer characteristics with internal heat generation in metal beads.

Experimental Apparatus:

The schematic diagram of the experimental apparatus is shown in Fig.(1), and the details of the test section is shown in Fig.(2). The air from the compressor tank (2) flows through the control valve (2) to the test section (1) across a flexible connection (4). The control valve is adjusted to permits the air to flow at a pressure of 1.3 bar. The test section is a copper flanged tube (1) with an inside diameter of 20 mm, wall thickness of 1 mm, and 225 mm length. The outside surface of the test section is electrically insulated with 1 mm thickness mica sheet (17), and is wrapped with the induction coil (13) (1 mm wire diameter, 8 Ω electric resistance).

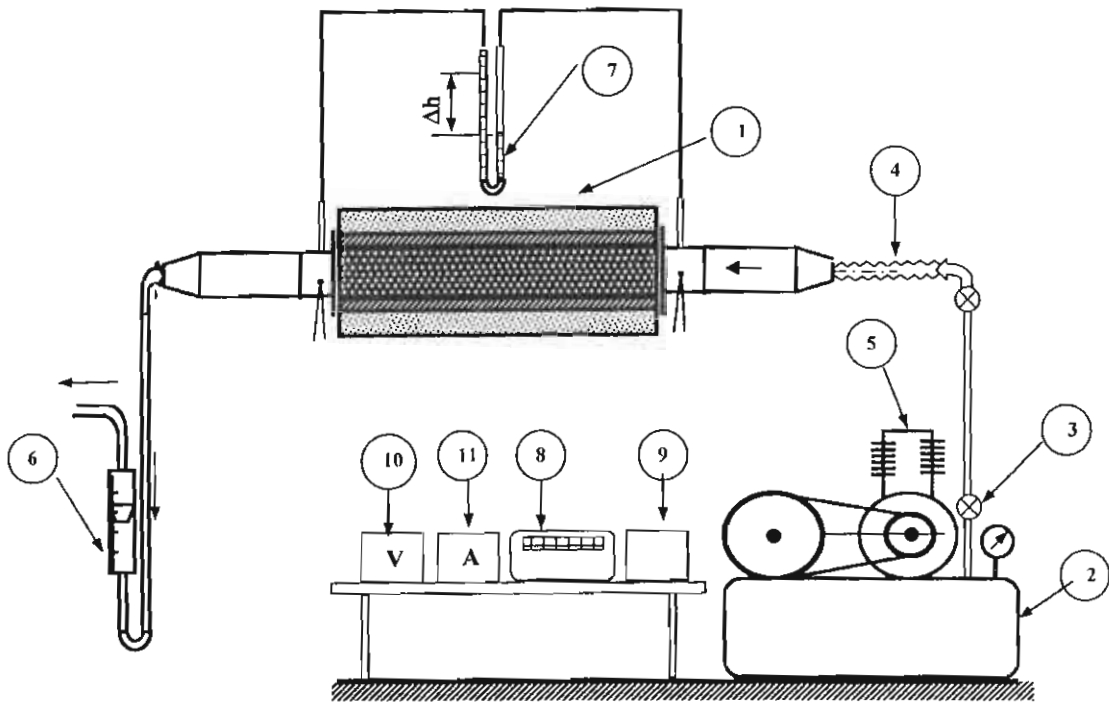
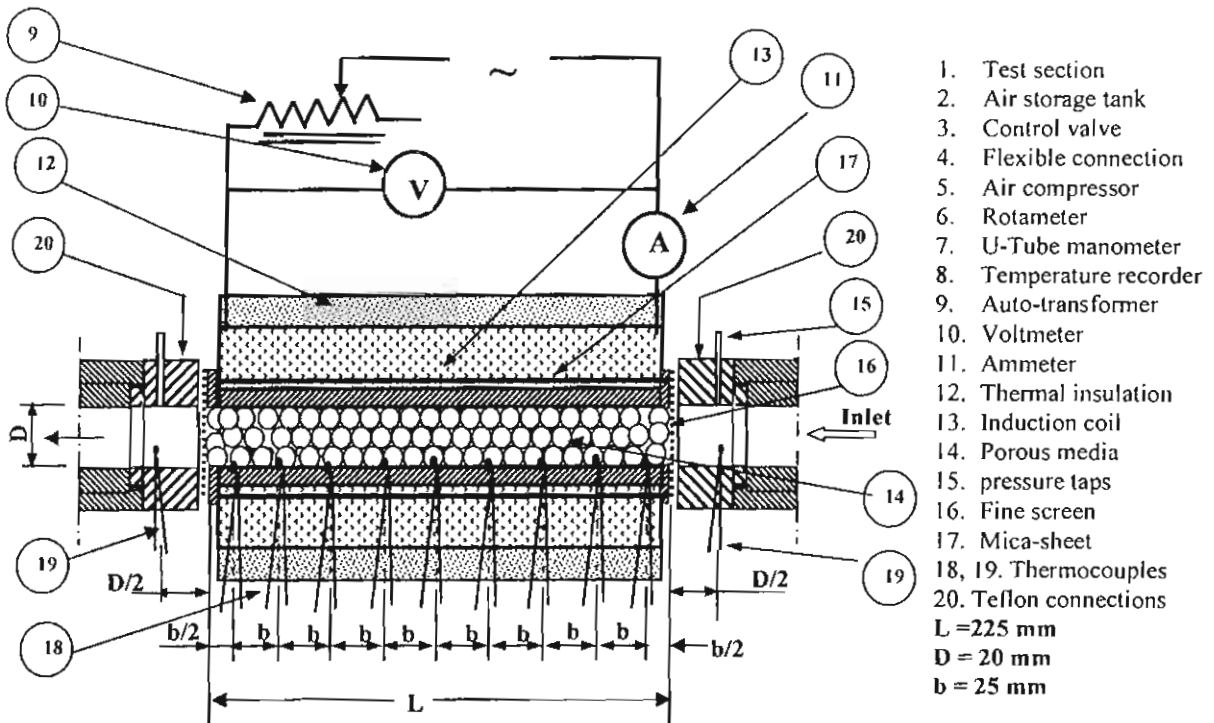


Fig.1 Schematic diagram of the test rig.



- 1. Test section
 - 2. Air storage tank
 - 3. Control valve
 - 4. Flexible connection
 - 5. Air compressor
 - 6. Rotameter
 - 7. U-Tube manometer
 - 8. Temperature recorder
 - 9. Auto-transformer
 - 10. Voltmeter
 - 11. Ammeter
 - 12. Thermal insulation
 - 13. Induction coil
 - 14. Porous media
 - 15. pressure taps
 - 16. Fine screen
 - 17. Mica-sheet
 - 18, 19. Thermocouples
 - 20. Teflon connections
- $L = 225 \text{ mm}$
 $D = 20 \text{ mm}$
 $b = 25 \text{ mm}$

Fig. 2 Details of test section .

Two pressure taps of 0.8 mm inside diameter (15) are located in the vicinity of the test section, 10 mm from inlet and outlet of the test section to measure the pressure drop across the porous media with the help of U-tube water manometer (7).

Spherical steel beads of uniform size (14) are randomly packed inside the test section and retained by a fine copper screens (16) fixed at either end of the test section. The diameters of steel beads investigated are 5, 6.5, 11, and 16 mm. Table(1) lists the characteristics of the samples that are used in the experiments. The porosity is the void volume fraction, the bead diameter is measured by a micrometer, and the number of pores in the test section is estimated by counting it.

Table (1): Geometry of porous media

d, mm	5	8	11	16
D/d	4.000	2.250	1.818	1.250
ϕ	0.2527	0.3552	0.4599	0.5251

The inside wall temperature of the test section is measured by nine copper-constantan thermocouples (18), 25 mm apart. To prevent the back conduction of heat from the heated to the unheated sections in the longitudinal direction, two teflon connections (20), are fixed at both inlet and outlet of the test section. Two thermocouples (19) are fitted at inlet and outlet of the test section at the midplane to measure the air temperature at inlet and outlet of the test section. The air temperature at inlet to the test section T_{in} was slightly higher than the ambient temperature, but always less than 2% of the maximum wall temperature, indicating that back conduction effects were negligible. The temperature readings indicated by the thermocouples were monitored until they reached steady state. The steady state condition of flow is reached after about 30 minutes depending on the flow velocity. It typically took longer at lower flow velocities. The temperature were monitored

for an additional interval of five minutes to ensure that steady state was assumed if the temperature did not vary more than 0.1°C during a five minutes interval. All thermocouples are connected to a temperature recorder (8) with accuracy of 0.1°C through a multi-switch points.

AC power supply is provided to the copper induction coil (13) which is controlled by a variac (9). The volt and electric current through the induction coil is measured by an voltmeter (10) and ammeter (11), respectively as shown in Fig.(2). Air flow rate is measured by a rotameter (6) and the average velocity of air flowing through the metal beads is then the average flow rate divided by the cross-sectional area of the test section.

The experimental error estimation can be made based on the accuracies for instruments which measure the individual quantities. The error (thermocouple calibration and resolution of the data acquisition device) in the estimation of T_{avg} is 0.3°C. Based on the published accuracies of the voltmeter and ammeter, the error in the estimate of the induction heat generation is 2%. The error in the estimate of the length, area, and volume are negligible because they are extremely low (<0.3% of the measured quantities).

2. Data Reduction:

The average porosity ϕ in the test section is defined from volumetric measurements for each size of the steal beads. The measured mean values of ϕ for the large, medium, and small size beads used are 0.2527, 0.3552, 0.4599, and 0.5251, respectively with an uncertainty of $\pm 1.2\%$.

From the some arbitrary definitions of the mean velocity u , friction factor f , and Reynolds number Re in the literatures [6, 10], the following relations are used in this study:

$$u = V_a / A_c \quad (1)$$

where \dot{V}_a is air volume flow rate, and A_c is the cross sectional area of the tested tube.

$$f = \frac{\Delta P}{\Delta L} \cdot \frac{d\phi^3}{\rho_a u^2 (1-\phi)} \quad (2)$$

$$Re = \frac{\rho u d}{\mu(1-\phi)} \quad (3)$$

The average wall temperature ΔT_{avg} is defined as:

$$\Delta T_{avg} = \frac{\sum_{i=1}^n T_{wi} - T_{in}}{n} \quad (4)$$

Where n is the number of thermocouples fixed on the inside wall of the test section.

The rate of induction heat generated through the spherical steel beads is calculated by:

$$Q = m_a C_p (T_{in} - T_{ex}) \quad (5)$$

The average heat transfer coefficient from the steel beads is defined as:

$$h = \frac{Q}{A \Delta T_{avg}} \quad (6)$$

Where Q is the rate of induction heat generated through the steel beads, A is the surface area of the steel beads, ($A = n \frac{\pi}{4} d_b^2$) and n is the number of beads which fill the test section.

The average Nusselt number is calculated by the relation:

$$Nu = \frac{h d_B}{k_a} \quad (7)$$

Where d_B is the diameter of the beads, and k_a is the air thermal conductivity.

3. Results and Discussion

3.1: Pressure Drop and Friction Factor

The relation between modified Reynolds number Re^* , and pressure drop at different values of porosity is shown in Fig.(3). The pressure drop increases with increasing Reynolds number at constant

values of porosity. The hydrodynamic boundary layer develops much more quickly in porous media due to lateral mixing caused by the channeling effect. It is interesting to note that at a constant Reynolds number, increasing porosity led to decrease the pressure drop.

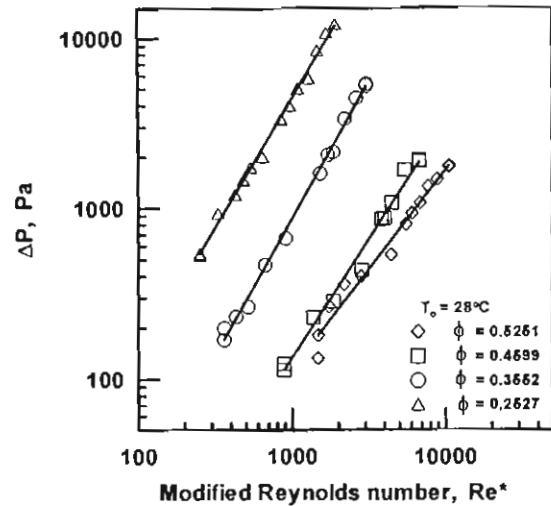


Fig. (3) Pressure drop versus the modified Reynolds number for various values of porosity.

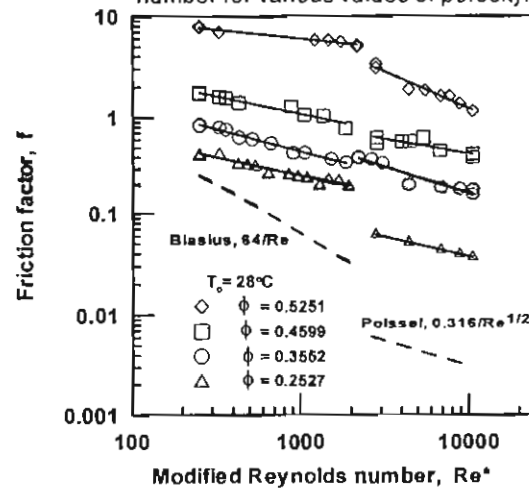


Fig.(4) Variation of present friction factor with modified Reynolds number for various values of porosity.

The friction factor as function of modified Reynolds number is shown in Fig.(4). It is clear that the friction factor decreases with increasing modified Reynolds number for different values of porosity, and also increases with increasing porosity at constant values of Reynolds number.

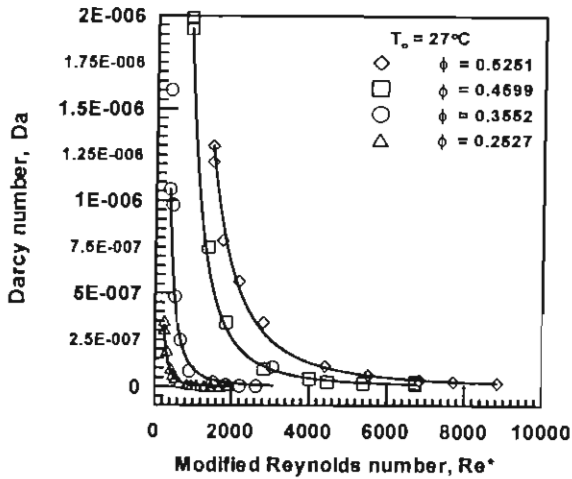


Fig.(5) The dependence of Darcy number on Reynolds number for different values of porosity.

Figure(5) shows the variation of Darcy number with the modified Reynolds number at constant values of porosity. It is obvious to note that Darcy number decreases dramatically with increasing Reynolds number until it reach a certain value after which the decrement in Darcy number is uniform. This is because the hydrodynamic boundary layer develops much more quickly in porous media due to the lateral mixing caused by the channeling effect.

3.2: Heat Generation and Flow Temperature:

As a variable magnetic field which results as passing AC current through the induction coil, the eddy current results tends to increase the beads internal energy and consequently raising its temperature. It depends on the coil geometry (no. of turns, length of coil, distance between each two turns) and magnetic permeability of the beads, [1]. The rate of heat generation through the steel beads equals the rate of heat gained by the fluid, $m_a C_p \Delta T_a$ which is less than the electric

power input to the induction coil depending upon flow velocity, medium permeability, and induction coil geometry. The results of dimensionless induction heat generation with Reynolds number is shown in Fig.(6). It is clear that the inducted heat generation (it depends on porosity, air velocity, permeability of the medium to the magnetic field, length of the induction coil, mean coil diameter and power input) increases with increasing Reynolds number. Also, the exit air temperature of the test section decreases with increasing Reynolds number.

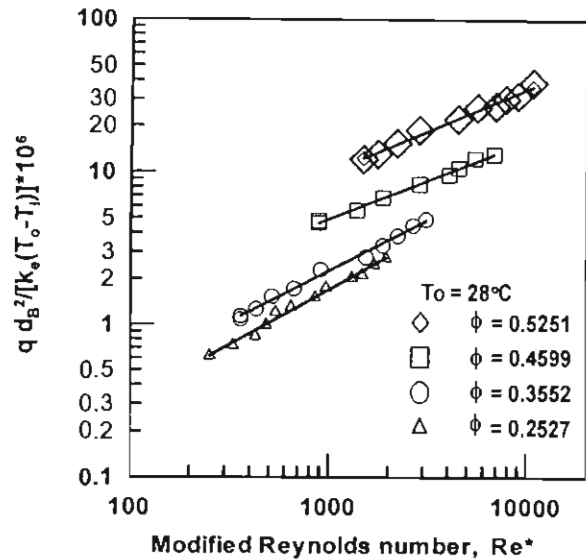


Fig.(6) variation of the dimensionless induction heat generation with modified Reynolds number at different values of porosity.

3.3: Effect of porosity on Heat Transfer Coefficient

Figure(7) shows the variation of Nusselt number with the forced convection strength, $Gr.Da/Re^2$ (forced convection dominated flow, natural convection dominated flow or mixed convection dominated flow).

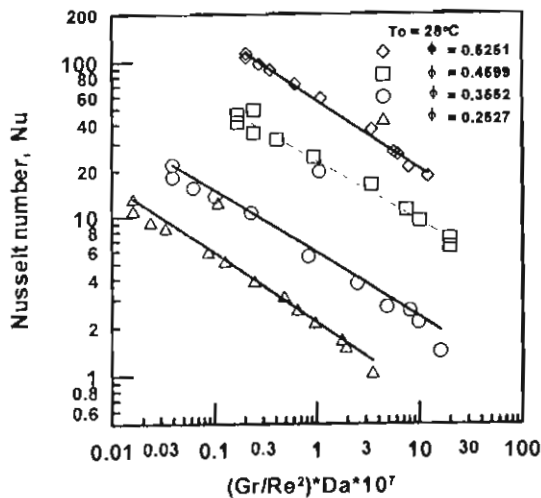


Fig. (7) Variation of the average Nusselt number on forced convection strength at different values of porosity.

It is clear that for all runs performed in this work, the average Nusselt number decreases with increasing the forced convection strength ($Gr.Da/Re^2$) $\ll 0.01$ [6], which suggests that the heat transfer data obtained are in forced convection dominated flow.

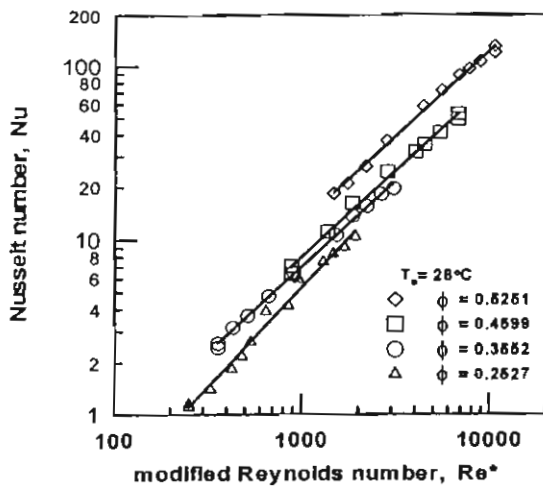


Fig. (8) Variation of Nusselt number with modified Reynolds number at different values of porosity.

Figure (8) shows a plot of average Nusselt number of the beads surface as a function of Reynolds number for different values of porosity. As expected, the average

Nusselt number increases with increasing both modified Reynolds number and porosity.

3.4: Effect of beads diameter to pipe diameter ratio

The behavior of Nusselt number with bead diameter/pipe diameter ratio is shown in Fig.(9) for $d_B = 5, 8, 11,$ and 16 mm and $Gr = 1.15 \times 10^7$. Increasing beads diameter to pipe diameter ratio causes an increase of Reynolds number which tends to an increase in Nusselt number. This is because the increase of beads diameter led to increase Reynolds number and channeling effect.

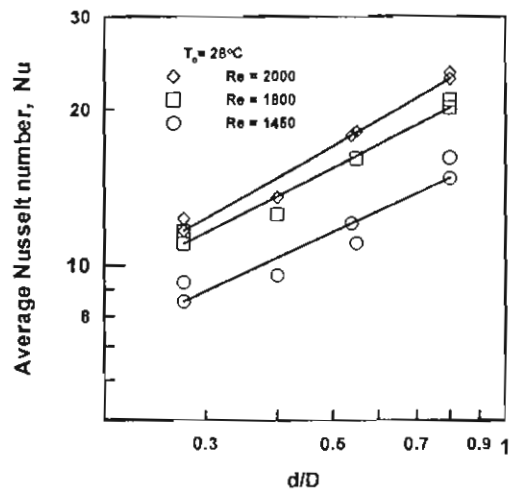


Fig.(9) Nusselt number versus beads diameter to test section diameter ratio at different values of Reynolds number.

4. Correlating of the Present Experimental Data

Comparison of the present experimental data with those in Literature is very difficult, due to the diversity in the experimental condition.

An attempt is made to correlate the present experimental data to obtain the dependence of friction factor with Re^* , Da , and (d/D) and the dependence of Nusselt number on Re^* , Ra , and (d/D) . By the mathematical statistical analysis (Least Squares method), a correlation for both friction factor and mean Nusselt number are correlated as follows:

$$f = 5.82067 \text{Re}^{-0.77946} \text{Da}^{-0.6391} \left(\frac{d}{D}\right)^{3.72364} \quad (8)$$

$$\text{Nu} = 0.02528 \text{Re}^{0.6375} \text{Ra}^{-0.1652} \left(\frac{d}{D}\right)^{1.4671} \quad (9)$$

These correlations are valid in the ranges $250 < \text{Re} < 10000$, $1.5 \times 10^{-9} < (\text{Gr} \cdot \text{Da} / \text{Re}^2) < 2.0 \times 10^{-6}$ and $1.2 \times 10^6 < \text{Ra} < 1.1 \times 10^7$

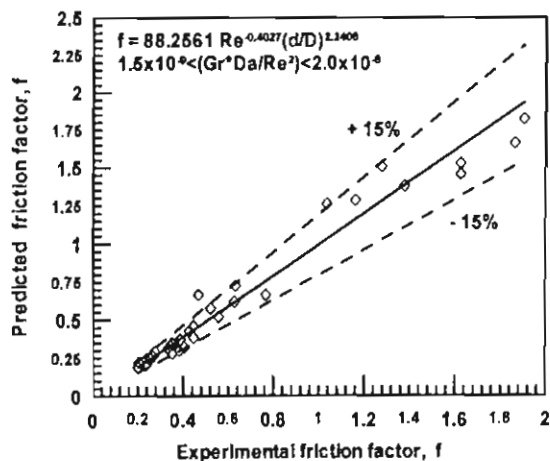


Fig. (10) Correlation of present experimental data of friction factor with the predicted results.

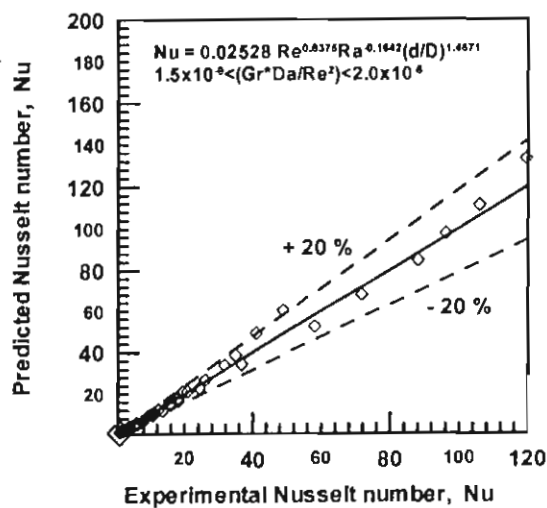


Fig. (11) Correlation of present experimental data of Nusselt number with the predicted values.

Figures (10) and (11) show the deviation between present experimental data and the present correlations. The deviation of present experimental data from these

correlations are $\pm 15\%$ for friction factor and $\pm 20\%$ for Nusselt number.

4. Conclusions:

Heat transfer characteristics of forced convection with heat generation through porous media is studied experimentally. The investigation is focused on the dependence of heat flow characteristics on Reynolds number, porosity, and Darcy number. The following conclusions are obtained:

- i. The heat transfer rate from the porous media increases with increasing the modified Reynolds number.
- ii. Nusselt number increases with increasing porosity
- iii. The friction factor decreases with increasing Reynolds number.
- iv. Darcy number decreases with increasing Reynolds number.
- v. The obtained correlations of both friction factor and average Nusselt number are a helpful tool in the selection of this type applications.

5. References:

1. B. L. Theraja, "A text Book of Electrical Technology", NIRAJ PRAKASHAN, New Delhi-55, 1971.
2. D. Moalem, "Steady State Heat Transfer Within Porous Medium with Temperature Dependent Heat Generation", Int. J. Heat Mass Transfer, Vol. 19, pp.529-537, 1976.
3. M. Tveitereid, "Thermal Convection in a Horizontal Porous Layer with Internal Heat Generation", Int. J. Heat Mass Transfer, Vol.20, pp.1045-1050, 1977.
4. N. Decker and L. R. Glicksman, "Heat Transfer in Large Particle Fluidized Beds", Int. J. Heat Mass Transfer, Vol.26, N0.9, pp.1307-1320, 1983.

5. I. Catton and J. O. Jakobsson, "The Effect of Pressure on Dryout of a Saturated Bed of Heat Generating Particles", ASME Trans., Journal of Heat Transfer, Vol.109, PP.185-195, 1987.
6. W. E. Stewart, L. Cai, and L. A. Stickler, "Convection in Heat Generating Porous Media with Permeable Boundaries – Natural Ventilation of Grain Storage Bins", ASME Transaction, Journal of Heat Transfer, Vol.116, pp.1044-1046, 1994.
7. D. Gobin, B. Goyeau and J. P. Songbe, "Double Diffusive Natural Convection in a Composite Fluid-Porous Layer", ASME Transaction, Journal of Heat Transfer, Vol.120, pp.234-241, 1998.
8. V. V. Calmidi and R. L. Mahajan, "Forced Convection in High porosity Metal Foams", ASME Transaction, Journal of Heat Transfer, Vol.122, pp.557-565, 2000.
9. R. bemacer, H. Beji, F. Oueslati, and A. Belghith, "Multiple Natural Convection Solution in Porous Media Under Cross Temperature and concentration Gradients", Numerical Heat transfer, Part A39, pp.553-567, 2001.
10. S. Y. Lee, 2001, "Heat Transfer Calculation for Normal Operations of a Fixed CST Bed column", WSRC – TR- 2001 – 00255, May 2001.
11. A. P. Mozhaev and V. M. Polyayev, "Study of Internal Heat Transfer in a Non-Uniform Porous Media", Heat Transfer Research, Vol.33, Nos.3 & 4, 2001.
12. A. R. Raffray, J. Pulsifer, and M. S. Tillack, Modeling Flow and Heat Transfer Through Porous Media for High Heat Flux Applications", Engineering Development and Technology 002 (UCEI), October 2002.
13. B. K. Rao, "Internal Heat Transfer to Power Low Fluid Flow Through Porous Media", Experimental Heat Transfer, Vol.15, PP.73-87, 2002.
14. A. Khalili, I.S. Shivakumara and M. Huettel, "Effect of Throughflow and Internal Heat Generation on Convective Instabilities in an Anisotropic Porous Layer", Journal of Porous Media, 5(3), 187-198, 2002.